Journal of Material Science and Mechanical Engineering (JMSME)
p-ISSN: 2393-9095; e-ISSN: 2393-9109; Volume 5, Issue 4; October-December, 2018, pp. 142-145

http://www.krishisanskriti.org/Publication.html

Synthesis and Characterization of Chlorine Doped Hydroxyapatite

Abreeq Naqshbandi[1]* and Atikur Rahman[2]

[1,2]Department of Metallurgy and Materials Engineering, NIT Srinagar, 190006, India
E-mail: [1]naqshbandiabreeq@gmail.com, [2]atikurrhmn@nitsri.net

Abstract—*The objective of the present study was to synthesize $Ca_{10}(PO_4)_6OH_{2-x}Cl_x$ nanoparticles by High Energy Ball Mill (Cryomill) for biomedical applications. Calcium Hydroxide ($Ca(OH)_2$), Calcium Chloride ($CaCl_2$, $2H_2O$) and Phosphorous Pentoxide (P_2O_5) were used as starting materials. XRD results confirmed that a single phase of Chloroapatite (ClAp) was formed by doping Chlorine ions (x = 2) into Hydroxyapatite and after milling from 2 to 8 hr. Crystallite size and lattice strain were considerably influenced by the increase in milling time. SEM was used to observe the surface morphology of the nanoparticles.*

1. INTRODUCTION

The use of bone grafts in dealing with problems associated with bone loss, repair, and reconstruction has been done since a long time. However recent researches have been conducted for investigating the materials that have the capability of initiating natural bone regeneration process from a damaged or lost bone tissue. Such materials remain in contact with the fluids and tissues of the body for extended periods of time. One of the major requirements of biomaterial is biocompatibility and bio-functionality. Biomaterials used as bone grafts are classified on the basis of osteogenicity (presence of bone forming cells), osteoconductivity (ability to function as a bone scaffold) and osteoinductivity (ability to stimulate bone formation) [1]. Calcium hydroxyapatite, $Ca_{10}(PO_4)_6(OH)_2$, commonly known as Hydroxyapatite (HA), is a synthetic biomaterial similar to biological HA, which forms the structural component of the human bone and teeth. It has been used widely for various bone and tooth implants due to its exemplary biocompatibility and bioactivity. Owing to these properties this bioactive ceramic is broadly applied as bone-fillers, bone tissue scaffolds, bioactive coatings and composites. They are also used for drug, protein, and gene delivery as well as fluorescence labeling, cell targeting, imaging materials [2]. The crystallinity, lattice parameters, and morphology of the apatite structure can be altered by doping anions and cations into the HA lattice [3], which inturn improve the stability, crystallinity and biocompatibility of Hydroxyapatite (HA). Chlorine ions (Cl^-) and fluorine ions (F^-) are widely considered as potential anion dopants because of their biological significance. The presence of chlorine ions in HA structure initiates osteoclast stimulation by making an acidic environment on the surface of bone during the bone resorption process [4]. Most of the researchers have reported the synthesis of chlorine doped HA via hydrothermal treatments [5], and aqueous precipitation method [6] . Very limited literature is available on synthesis of chlorine doped HA by high energy ball mills. Therefore the aim of the present research work is to study the effect of ball milling time on the crystal structure and biocompatibility of chlorine doped HA [$Ca_{10}(PO_4)_6OH_{2-x}Cl_x$].

2. EXPERIMENTAL

2. 1 Materials and methods

$Ca_{10}(PO_4)_6$ $(OH)_{2-x}Cl_x$ (x= 0,2) nanoparticles were synthesized in the laboratory using High Energy Ball Mill (Cryomill, KC-0, Tau Instruments, India). High purity chemicals (99% purity) viz; Calcium Chloride Dihydrate ($CaCl_2$. $2H_2O$, Rankem), Phosphorus Pentoxide (P_2O_5, Thomas Baker), Calcium Hydroxide ($Ca(OH)_2$, Thomas Baker) were used as starting materials with Calcium Chloride being the dopant source. The above chemicals were used without any further purification. Appropriate amount of chemicals were mixed using High Energy Ball Mill. The schematic of the cryomill used for the synthesis is shown in fig 1. The milling operation was performed under liquid nitrogen atmosphere. The molar ratio of Calcium Hydroxide to Phosphorous Pentoxide and Calcium Chloride was 10:3:0, 9.75:3:0.25, 9.5:3:0.5, 9.25:3:0.75 and 9:3:1 for x = 0.0, 0.5, 1.0, 1.5, and 2.0 respectively. But here we have reported for x = 0 and 2 only. Standard conditions for synthesizing $Ca_{10}(PO_4)_6$ $(OH)_{2-x}Cl_x$ (x = 0 , 2) nanoparticles are shown in Table 1. Ball to powder ratio was maintained at 25:1 and milling operation was performed with single hardened steel ball. Synthesized samples were heat treated in muffle furnace at 800 °C for 1 hr in air atmosphere. The heating rate of the furnace was 10 °C min^{-1}.

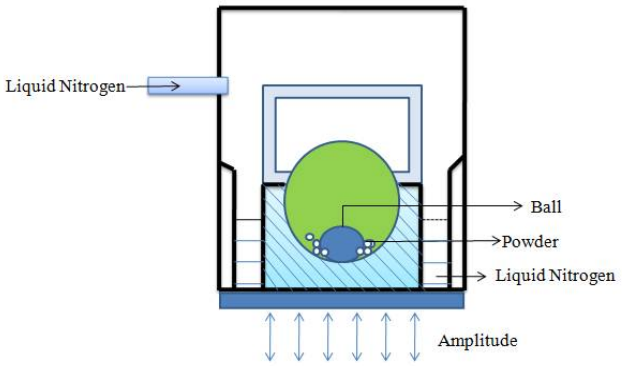

Fig. 1: Schematic diagram of High Energy Ball Mill

Table 1: Standard conditions for synthesis of $Ca_{10}(PO_4)_6(OH)_{2-x}Cl_x$ (x=0,2) nanoparticles

Mole Fraction (x)	Calcium-Phosphorus	Phosphorus Pentaoxide	Calcium Chloride	Milling Time
0	10	3	0	2
2	9	3	1	2,4,6,8

2.2 Characterization

XRD **(XPERTPro, PANalytical JDX-8030, JEOL)** measurements were made using CuK_α radiation to characterize the samples. The samples were scanned with a scan rate of 0.02^o/s in the scan range of 15 to 60^o. An average grain size of the samples was done by using its XRD peak broadening according to Scherrer formula [8] as given in Eq. (1).

$$D = \frac{0.9\lambda}{B\cos\theta} \quad (1)$$

where D is the average size of crystallite, B is the broadening of the diffraction line measured at half maximum intensity, λ is the wavelength of the X-ray radiation (1.54052 Å, CuK_α) and θ is the Bragg angle. The instrumental broadening has been considered for the calculation of grain size, and the value of 0.1 is subtracted (calculated using standard silicon sample) from the full-width half maximum (FWHM) value (B value).

The surface morphology and the composition of Ca,P, O and Cl were determined by FE-SEM / EDS ((FEI, Quanta 200F)) energy dispersive X-ray spectrometer on K and L lines and operated at an accelerated voltage of 20 kV. EDAX Genesis 32 software was used to calculate the elemental composition of the powders.

3. RESULTS AND DISCUSSION

3.1 X-ray diffraction (XRD)-Structural studies

The typical X-ray diffraction peaks of chlorine doped HA [$Ca_{10}(PO_4)_6OH_{2-x}Cl_x$, where x = 0 & 2) nanoparticles are given in Fig. 1. (a). XRD patterns of these samples exhibit peaks corresponding to (110), (200), (201), (002), (210), (211), (112), (202), (301), (212), (221), (131), (400), (222), (230), (213), (321), (303) and (322) planes, which can be indexed as the Chloro apatite (ClAp) according to File Number: PDF# 861203. There were no detectable diffraction peaks of any impurity phases within the sensitivity of our XRD measurements, implying that Cl ions was incorporated into the hydroxyapatite lattice sites. In addition, compared to un-doped hydroxyapatite nanoparticles, increasing Cl doping concentration caused a shift in diffraction peak position of the Chlorine doped hydroxyapatite nanoparticles. Table 2 shows the mean crystallite size and lattice strain that was determined from the broadening of the diffraction peaks using Debye–Scherer's formula [8]. Fig 1 shows the XRD patterns of the samples synthesized at different milling times.

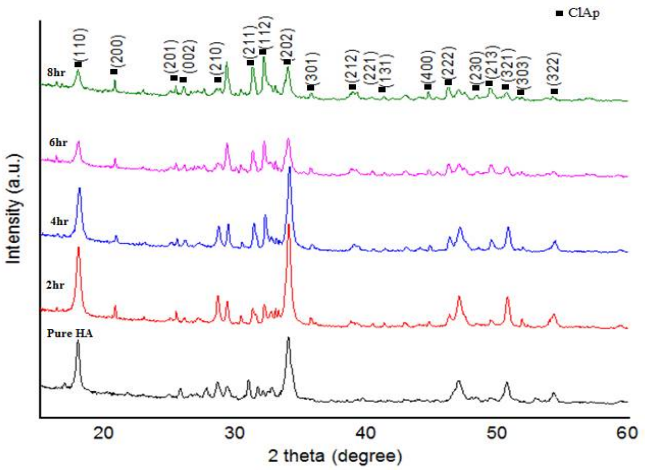

Fig. 1: XRD traces of ClAp powders at different milling times

The effect of milling time under on crystallite size of prepared ClAp samples is shown in Fig. 2.

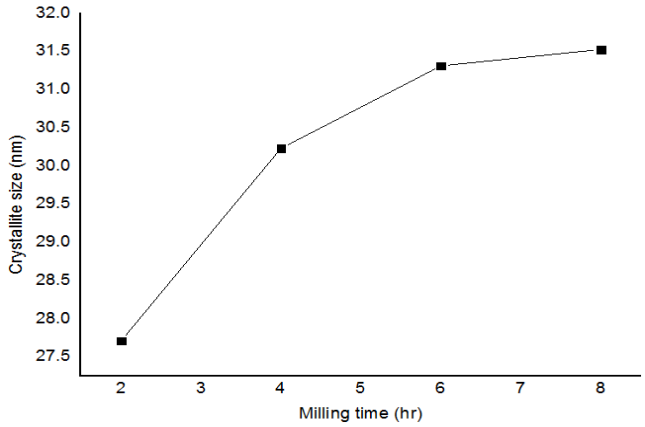

Fig. 2: The effect of milling time on the crystallite size

Table 2: Crystallite size and lattice strain of $Ca_{10}(PO_4)_6(OH)_{2-x}Cl_x$ (x = 0, 2) nanoparticles

Mole Fraction (x)	Milling time	Crystallite size (nm)	Lattice Strain (%)
0	2 hr	34.9	0.004875
2	2 hr	27.707	0.00595
2	4 hr	30.23	0.0056
2	6 hr	31.31	0.005275
2	8 hr	32.91	0.005175

It can be seen that as the milling time increased for Cl doped HA ($Ca_{10}(PO_4)_6$ Cl_2) nanoparticles, the crystal size increases slightly. This result is in agreement with the previos work conducted by Fathi *et al* [9]. But if we compare the undoped HA with Cl doped HA(($Ca_{10}(PO_4)_6$ Cl_2), the overall crystallite size of Cl doped HA ($Ca_{10}(PO_4)_6$ Cl_2) nanoparticles decreased. The corresponding lattice strain with respect to milling time due to the incorporation of Cl^- ions in the Hydroxy apatite structure is shown in Fig 3.

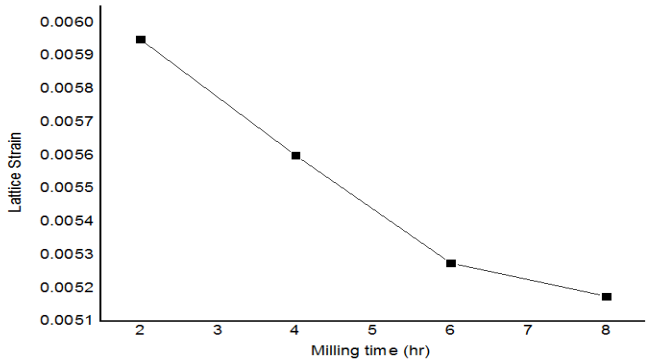

Fig. 3: The effect of milling time on the lattice strain

3.2 Microstructural and Compositional studies

The FE-SEM micrographs of Ca10(PO4)6OH2-xClx where (x = 0 & 2) nanoparticles are shown in Fig. 4 (a-e). It consists of loosely aggregated spheroid-like particles. Fig.4 (a) shows the micrograph of undoped hydroxyapatite (HA) nanoparticles depicting a slightly bigger particle size, which is also confirmed by the XRD data shown in Table 2. Fig.4 (b) corresponding to $Ca_{10}(PO_4)_6Cl_2$ (chloroapatite) (for x=2) nanoparticles with a milling time of 2hr depicts a smaller particle size compared to $Ca_{10}(PO_4)_6Cl_2$ (chloroapatite) (for x=2) nanoparticles milled for 4hr Fig.4(c), 6hr Fig.4 (d) and 8 hr Fig.4 (e). Reason of slightly increase in the size of the particles with an increase in the milling time might be due to good tendency to form clusters because of the large surface area of the partciles and van der Waals interactions [10]. During mechano-chemical activation, two particles share common crystallographic orientation when two neighbour primary particles collide. As a result, two particles combine into a secondary one so that the agglomeration can be continued [11].

Chemical compositions of undoped and Cl doped Hydroxy apatite ($Ca_{10}(PO_4)_6$ Cl_2) nanoparticles were investigated by EDS. The EDS spectra of undoped Hydroxyapatite and Cl doped Hydroxyapatite ($Ca_{10}(PO_4)_6$ $(OH)_{2-x}$ Cl_x) nanoparticles for x= 2 in Fig. 4(f) and (g) shows the existence of Ca, O, P and, Cl within the samples.

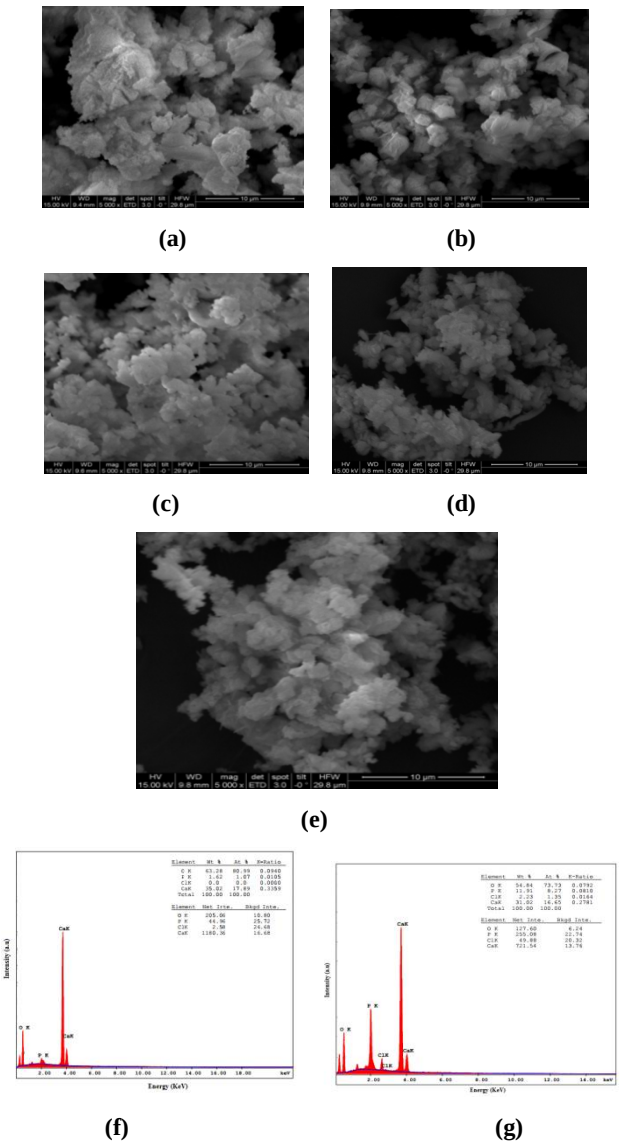

Fig. 4. FE-SEM photomicrographs of the milled samples: a) un-doped Hydroxyapatite, b) Cl doped hydroxyapatite($Ca_{10}(PO_4)_6$ Cl_2 milled for 2 hr c) milled for 4 hr d) milled for 6 hr e) milled for 8 hr f) EDS spectra of undoped Hydroxyapatite and g) Cl doped Hydroxyapatite

In this study we observed the following:

i) Doping Cl ions into hydroxyl apatite retards the grain growth, as it occupies the grain boundary of hydroxy apatite. It has been confirmed by XRD analysis (particle size calculation).
ii) Further, particle size of Cl doped hydroxyapatite ($Ca_{10}(PO_4)_6\ Cl_2$) was decreased by milling operation, but by increasing the milling time there was a slight increase in particle size. It might be due to good tendency to form clusters because of the large surface area of the partciles and van der Waals interactions [10]. Overall particle size of $Ca_{10}(PO_4)_6\ Cl_2$ nanoparticles was decreased by doping as well as by milling, which indicates the improvement in crystal structure which is required for good biocompatibility.
iii) Biocompatibility analysis will be done by simulated body fluid (SBF) tests.

4. CONCLUSION

The effect of milling time on the size and morphological feature of Cl doped hydoxyappatite ($Ca_{10}(PO_4)_6Cl_2$) nanoparticles was investigated. The crystallite size and lattice strain of the nanopartilces was strongly influenced by the milling time. The results revealed that crystallinity increased by doping as well as milling for 8hrs. XRD results revealed that Cl ions have been incorporated into host Hydoxyapatite matrix without altering the structure of hydoxyapatite. SEM images depicted accumulated fine agglomerates of the nanoparticles.

REFERENCES

[1] K. Ozer and K. C. Chung, "The Use of Bone Grafts and Substitutes in the Treatment of Distal Radius Fractures," *Hand Clinics*, vol. 28, no. 2. pp. 217–223, 2012.
[2] K. Lin, C. Wu, and J. Chang, "Advances in synthesis of calcium phosphate crystals with controlled size and shape," *Acta Biomaterialia*, vol. 10, no. 10. pp. 4071–4102, 2014.
[3] S. Kannan, A. Rebelo, and J. M. F. Ferreira, "Novel synthesis and structural characterization of fluorine and chlorine co-substituted hydroxyapatites," *J. Inorg. Biochem.*, vol. 100, no. 10, pp. 1692–1697, 2006.
[4] B. Nasiri-Tabrizi, A. Fahami, and R. Ebrahimi-Kahrizsangi, "Phase transitions and structural changes of nanostructured chlorapatite under thermal treatment," *Ceram. Int.*, vol. 40, no. 1 PART A, pp. 901–910, 2014.
[5] J. C. Rendón-Angeles, K. Yanagisawa, N. Ishizawa, and S. Oishi, "Effect of metal ions of chlorapatites on the topotaxial replacement by hydroxyapatite under hydrothermal conditions," *J. Solid State Chem.*, vol. 154, no. 2, pp. 569–578, 2000.
[6] S. Kannan, J. H. G. Rocha, and J. M. F. Ferreira, "Synthesis of hydroxy-chlorapatites solid solutions," *Mater. Lett.*, vol. 60, no. 7, pp. 864–868, 2006.
[7] A. Fahami, B. Nasiri-Tabrizi, and R. Ebrahimi-Kahrizsangi, "Mechanosynthesis and characterization of chlorapatite nanopowders," *Mater. Lett.*, vol. 110, pp. 117–121, 2013.
[8] D. Zou, D. Yan, L. Xiao, and Y. Dong, "Characterization of nanostructured TiN coatings fabricated by reactive plasma spraying," *Surf. Coatings Technol.*, vol. 202, no. 10, pp. 1928–1934, 2008.
[9] M. Kheradmandfard and M. H. Fathi, "Fabrication and characterization of nanocrystalline Mg-substituted fluorapatite by high energy ball milling," *Ceram. Int.*, vol. 39, no. 2, pp. 1651–1658, 2013.
[10] P. Baláž, *Mechanochemistry in nanoscience and minerals engineering*. 2008.
[11] C. Suryanarayana, "Mechanical alloying and milling," *Progress in Materials Science*, vol. 46, no. 1–2. pp. 1–184, 2001.